# Role of ATP and $P_i$ in the mechanism of insulin secretion in the mouse insulinoma $\beta$TC3 cell line

Klearchos K. PAPAS*‡, Robert C. LONG, Jr.†, Ioannis CONSTANTINIDIS†§ and Athanassios SAMBANIS*

*School of Chemical Engineering and Parker H. Petit Institute for Bioengineering and Bioscience, Georgia Institute of Technology, Atlanta, GA 30332, U.S.A., and †Frederik Philips Magnetic Resonance Research Center, Department of Radiology, Emory University School of Medicine, Atlanta, GA 30322, U.S.A.

Understanding the biochemical events associated with glucose-stimulated insulin secretion by pancreatic $\beta$ cells is of importance in gaining insight into both the pathophysiology of diabetes and the development of tissue-engineered bioartificial pancreatic substitutes. We have investigated the effects of glucose concentration on the bioenergetic status and on the metabolic and secretory functions exhibited by mouse insulinoma $\beta$TC3 cells entrapped in calcium alginate/poly-L-lysine/alginate (APA) beads. Cells entrapped in APA beads constitute a possible implantable bioartificial pancreas for the long-term treatment of insulin-dependent diabetes mellitus. Our results show that, in entrapped $\beta$TC3 cells, the oxygen consumption rate and the intracellular nucleotide triphosphate levels are unaffected by a step change in glucose concentration from 16 mM to 0 mM for 4.5 h and then back to 16 mM. The intracellular $P_i$ level and the ammonia production rate were doubled, while insulin secretion was decreased 10-fold, upon switching from 16 mM to 0 mM glucose. The implications of these findings in the context of pancreatic $\beta$ cell biochemistry and the mechanism of the 'Fuel Hypothesis' are discussed.

## INTRODUCTION

The biochemical events associated with glucose-stimulated insulin secretion in pancreatic $\beta$ cells are the subject of intense investigation for two important reasons. First, an understanding of the biochemistry of $\beta$ cells is expected to offer insight into the pathogenesis of diseases related to glucose homoeostasis. Secondly, this knowledge will be valuable in the development of tissue-engineered constructs for insulin delivery and thus in the long-term treatment of insulin-dependent diabetes mellitus.

A commonly used construct consists of insulin-secreting cells encapsulated in an alginate/poly-L-lysine/alginate (APA) permselective membrane. The membrane imposes a molecular mass cut-off of approx. 50 kDa; thus it allows low-molecular-mass nutrients and metabolites, including insulin, to pass through, but it excludes high-molecular-mass antibodies and cytotoxic cells. Thus encapsulation immunoprotects the cells post-implantation. Cells used in previous studies have included islets isolated from animal glands [1–5], as well as transformed $\beta$ cells [6–8] such as cells from the $\beta$TC family of mouse insulinomas [9]. The main advantage of using transformed cells is that, contrary to their normal counterparts, they can be amplified in culture to virtually any population size in a reproducible fashion and with relative ease. Thus transformed $\beta$ cells relax the cell availability limitation that exists with primary cells. On the other hand, there is a paucity of information concerning the biochemistry of these cells in the context of glucose-stimulated insulin secretion within implantable bioartificial tissue constructs.

For normal $\beta$ cells, there is substantial evidence to suggest that glucose-stimulated insulin secretion does not involve a direct interaction of glucose with a specific cell receptor; instead, stimulated secretion requires that glucose be metabolized before it is recognized as a secretagogue [10–12]. This has led to the formulation of the 'Fuel Hypothesis', which links glucose metabolism with the electrophysiological events associated with insulin release [13]. In mammalian islets this mechanism is postulated to proceed as follows. Elevation of the extracellular glucose concentration leads to an increase in the rate of glucose consumption, which in turn increases the rate of oxygen consumption and the levels of available ATP-related compounds (in the form of ATP or ATP/ADP or ATP/ADP·$P_i$). This increase in ATP-related ratios is thought to act directly on the ATP-sensitive $K^+$ channels, closing them. Closure of the $K^+$ channels results in the depolarization of the cell membrane, which in turn opens voltage-gated $Ca^{2+}$ channels, thus allowing an influx of $Ca^{2+}$ ions into the cell. The resulting elevated intracellular $Ca^{2+}$ concentration appears to be the ultimate messenger for insulin secretion. Experimental data used in formulating this mechanism were collected using isolated animal islets. Reported results exhibit significant differences, especially with regard to the role of ATP, due to differences in experimental conditions, culture-to-culture variations and changes induced by extraction procedures used for the conventional measurement of intracellular compounds.

The growth *in vitro* of transformed $\beta$ cells to large population sizes permits the use of NMR spectroscopy to investigate cellular biochemistry. The main advantage of NMR is the ability to monitor the same cell preparation repetitively over a prolonged period of time, thus preventing the possible experimental pitfalls associated with invasive techniques [14]. A commonly used NMR nucleus in studies of cellular bioenergetics is $^{31}P$. Metabolites detectable by $^{31}P$ include nucleotide triphosphates

Abbreviations used: APA, alginate/poly-L-lysine/alginate; DMEM, Dulbecco's modified essential medium; IRP, insulin-related peptide(s); $P_{i(total)}$, $P_{i(in)}$ and $P_{i(out)}$, total, intracellular and extracellular $P_i$ respectively; $t_1$, longitudinal relaxation time; $t_2$, spin-spin relaxation time.

‡ Present address: Sandoz Pharmaceuticals, East Hanover, NJ 07936, U.S.A.

§ To whom correspondence should be addressed: Emory University, Department of Radiology, 1364 Clifton Road NE, Room AG12, Atlanta, GA 30322, U.S.A.

(NTPs), which are primarily attributable to ATP [15], $P_i$ and intermediates in phospholipid metabolism.

In the present study, we have investigated the effects of glucose concentration on the bioenergetic status and on specific metabolic and secretory rates of $\beta$TC3 cells entrapped in APA beads. Relevant phosphates were measured by NMR, and nutrient and metabolite concentrations by conventional off-line techniques. This work forms the basis for an extensive study of the biochemical events associated with insulin secretion from pancreatic $\beta$ cell lines in a realistic immunoprotective environment.

## MATERIALS AND METHODS

### Cells and cell entrapment

Mouse insulinoma $\beta$TC3 cells [9] were obtained from the laboratory of Dr. Shimon Efrat, Department of Molecular Pharmacology, Albert Einstein College of Medicine, Bronx, NY, U.S.A. Cells were cultivated as monolayers in T-flasks in growth medium consisting of Dulbecco's modified essential medium (DMEM; P/N D-5648; Sigma Chemical Co., St. Louis, MO, U.S.A.) containing 25 mM glucose and supplemented with L-glutamine to a final concentration of 6 mM, 15% (v/v) heat-inactivated horse serum, 2.5% (v/v) fetal bovine serum and 1% (v/v) penicillin/streptomycin solution that consisted of 10000 units of penicillin and 10 mg/ml streptomycin (all from Sigma). Cultures were maintained at 37 °C in a humidified 5% $CO_2$/95% air atmosphere, and were passaged every 5–10 days. Cells from passage numbers 34–42 were used in all experiments.

Cells were entrapped in APA beads as described previously [7,16]. A total of 20 T-flasks of 175 $cm^2$ surface area each were used for every preparation. Flasks were treated with trypsin in groups of three. To prevent cell aggregation during the trypsinization procedure, the cell suspension from each treated T-flask was transferred to a spinner flask and stirred at 60 rev./min until the end of the procedure. For entrapment, cells were separated from the medium by mild centrifugation, and then resuspended in 2.0% (w/v) sodium alginate (Kelco LV, San Diego, CA, U.S.A.). Suspension droplets were allowed to fall into a 1.1% (w/v) $CaCl_2$ solution, producing calcium alginate beads containing entrapped cells. Beads were maintained for 1 day in growth medium in a spinner flask, and then treated with 2-(*N*-cyclohexylamino)ethanesulphonic acid, poly-L-lysine and alginate to form APA beads. Beads were $0.95 \pm 0.2$ mm (mean $\pm$ S.D.) in diameter, and contained initially $7 \times 10^7$ cells/ml of alginate.

Cell numbers and viability were measured using the Crystal Violet/citric acid and Trypan Blue staining methods respectively [6,7].

### Perfusion system

The perfusion system used for the NMR experiments is shown in Figure 1. Beads with entrapped cells were placed in a 22 ml packed-bed bioreactor, resulting in a total number of $1.5 \times 10^9$ cells at the beginning of each experiment. The perfusion system consisted of three loops for the circulation of medium: (1) a perfusion loop, in which medium was circulated continuously at a rate of 30 ml/min from a medium reservoir through the bioreactor and back into the medium reservoir; (2) a medium replenishment loop, which was used to replace spent medium in the medium reservoir with fresh growth medium; and (3) a medium switching loop, which allowed for the rapid exchange of media in the medium reservoir. In the experiments described here, the medium switching loop was used to accomplish the step changes in glucose concentration. The bioreactor was bracketed by temperature sensors (Resistance Temperature Devices; Omega Engineering, Inc., Stamford, CT, U.S.A.) and polarographic dissolved-oxygen probes (Ingold, Wilmington, MA, U.S.A.) in flow-through cells. All sensors were interfaced to a personal

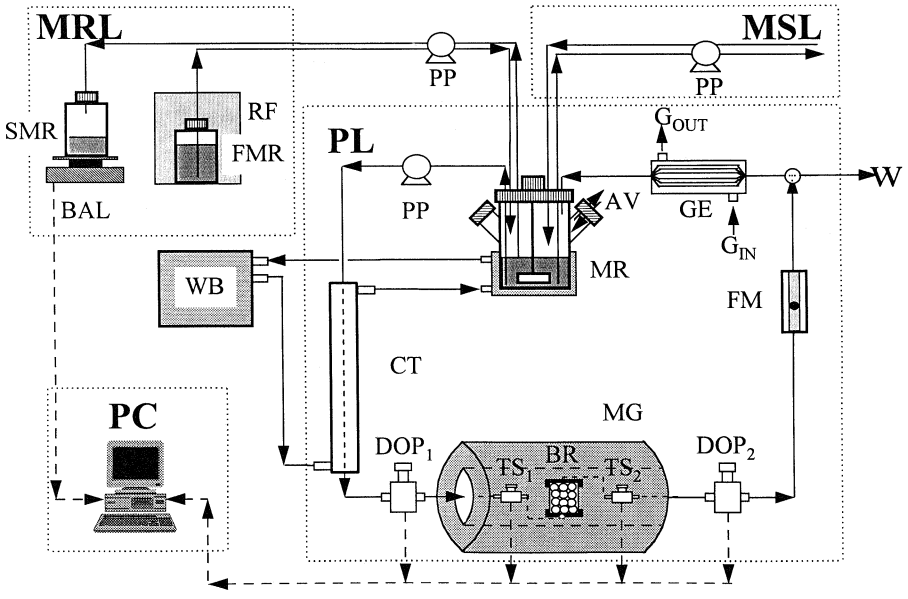


**Figure 1 Perfusion system used for NMR studies with entrapped $\beta$TC3 cells**

Abbreviations: AV, air vent; BAL, balance; BR, packed-bed bioreactor; CT, coaxial heat exchanger; $DOP_1$ and $DOP_2$, polarographic dissolved-oxygen probes in flow-through cells; FM, flow meter; GE, gas exchanger; FMR, fresh-medium reservoir; $G_{IN}$ and $G_{OUT}$, gas inlet and outlet respectively; MG, magnet of NMR spectrometer; MR, medium reservoir; MRL, medium replenishment loop; MSL, medium switching loop; PC, personal computer with data acquisition software; PL, perfusion loop; PP, peristaltic pump; RF, refrigerator; SMR, spent-medium reservoir; $TS_1$ and $TS_2$, resistance temperature sensors in flow-through cells; W, waste stream; WB, water-bath.

computer via an analog-to-digital board for repetitive data acquisition. A coaxial heat exchanger was used to control the temperature of the medium entering the bioreactor. The concentration of dissolved oxygen in the medium was maintained by pumping incubator air through the head space of the medium reservoir.

To initiate the experiment, the perfusion system was loaded with fresh growth medium and operated batchwise (without replenishment) until the glucose concentration had dropped to approx. 16 mM. Medium replenishment was initiated at a rate that maintained the residual glucose concentration in the perfusion loop at 16 mM (maintenance conditions). Fresh growth medium was pumped out of a refrigerated reservoir into the medium reservoir, and spent medium was withdrawn from the medium reservoir with a peristaltic pump. Medium volume in the medium reservoir was kept constant by positioning the medium withdrawal tube at a fixed level above the bottom of the flask. The output of spent medium was measured by weight using an electronic balance interfaced to the data acquisition system.

To perform a zero-glucose episode, medium replenishment was stopped and perfusion through the bioreactor was interrupted for 1.5 min. During this time, the high-glucose medium was removed from the medium reservoir and saved in a collection bottle. This medium was used later to re-establish maintenance operation after the zero-glucose episode was completed. A 1 litre volume of zero-glucose DMEM (P/N D-5030; Sigma) pre-equilibrated with incubator air (95 % air/5 % $CO_2$) at 37 °C was then pumped into the medium reservoir at a rate of 200 ml/min. The two media were confirmed to be of the same pH by withdrawing samples immediately before the medium switch and measuring the pH. To ensure complete removal of the 16 mM glucose medium from the perfusion loop, the zero-glucose medium was allowed to flow in single-pass mode through the bioreactor into a waste bottle for 25 min; medium recirculation was then started. Care was taken to avoid the introduction of air bubbles into the bioreactor during this procedure. The perfusion system was operated batchwise for the duration of each zero-glucose episode. The reverse steps were performed to switch from zero-glucose to 16 mM glucose medium.

### NMR spectroscopy

$^{31}P$ NMR spectra were obtained with a horizontal-bore SISCO 200/33 spectrometer operating at 200.057 MHz for $^{1}H$ and 80.984 MHz for $^{31}P$. The usable diameter of the bore was 12.5 cm. Data were acquired using a double-tuned $^{31}P/^{1}H$ home-built probe based on the modifications proposed by Chang et al. [17] to the original design of Schnall et al. [18]. The radio-frequency antenna consisted of a loop-gap resonator that surrounded the cylindrical shape of the bioreactor. Typical acquisition parameters for the $^{31}P$ experiments were: 3000 Hz spectral width, 4096 complex points per free induction decay, 512 transients, 90° pulses, and 3 s inter-pulse delays. Longitudinal relaxation time ($t_1$) measurements were performed using an inversion recovery pulse sequence with the following acquisition parameters: 3000 Hz spectral width, 4096 complex points per free induction decay, 1024 transients, and 4 s relaxation delay; the inversion time varied between 0 and 3.0 s.

A 0.049 ml capillary tube containing trisodium trimetaphosphate at a concentration of 97 mM was placed within the bioreactor and used as a concentration reference. Due to the long $t_1$ of trimetaphosphate (greater than 10 s), a water solution of Gadodiamide and Caldiamide (Omniscan®; Sanofi Winthrop Pharmaceuticals, New York, NY, U.S.A.) was added to the trimetaphosphate solution; this lowered $t_1$ to $0.14 \pm 0.01$ s.

All $^{31}P$ NMR spectra were processed using an 8 Hz exponential line-broadening filter prior to Fourier transformation. Acquired spectra were simulated in the frequency domain using a Lorentzian fitting routine (Varian, Palo Alto, CA, U.S.A.). Ratios of observed metabolites to trimetaphosphate were determined based on the fitted values of the areas under the peaks.

### Analytical techniques

Lactate and ammonia concentrations were measured using a Kodak Ektachem DT60II Analyzer (Eastman Kodak, Rochester, NY, U.S.A.). Glucose concentration was measured either with the Kodak Ektachem DT60II Analyzer or with an enzymic spectrophotometric kit (Trinder reagent; Sigma). Insulin was assayed by liquid-phase radioimmunoassay (Ventrex, Portland, ME, U.S.A.). The kit employed a polyclonal guinea-pig antiserum against pig insulin and pig insulin standards. The antiserum had 100 % reactivity against human and pig insulin, 33 % cross-reactivity with proinsulin and no reactivity with pig C peptide (manufacturer's data). Since the antiserum reacted with both proinsulin and insulin, the immunoreactive peptides assayed with the kit are collectively referred to as insulin-related peptides (IRP). Intracellular ATP was measured in monolayer cultures by a spectrophotometric enzymic method (P/N 366-UV; Sigma) in cells that were trypsin-treated and lysed by sonication.

### Monolayer studies

All monolayer cultures were fed with growth medium before each experiment. Eight flasks, separated into two groups of four flasks each, were used in these experiments. At confluency, the flasks were each fed for 4 h with 20 ml of serum-free DMEM containing 0 mM or 25 mM glucose. Media samples were collected from each flask at the beginning and at the end of the 4 h interval to determine the concentrations of glucose, lactate, ammonia and IRP. Intracellular ATP measurements were performed at the end of the 4 h exposure.

## RESULTS

NMR experiments were begun 24 h after completion of the entrapment protocol and lasted for 5 days. Three independent cultures were used in the experiments described in this study. Entrapped $\beta$TC3 cells were exposed to 0 mM glucose four times in two cultures, and twice in the third culture. Each zero-glucose episode lasted for 4.5 h, and the cells were allowed to recover in high-glucose medium for at least 16 h. $^{31}P$ NMR spectra were acquired every 27 min throughout the study. Aliquots of the perfusion medium were withdrawn for glucose, lactate, ammonia and IRP analyses.

The viability of $\beta$TC3 cells was measured at three time points during these experiments: once with freshly trypsinized cells, a second time after completion of the entrapment protocol (day 0), and finally at the end of the experiment (day 5). The average viability declined from $96.2 \pm 1.9$ % in freshly trypsinized cells to $90.7 \pm 2.3$ % at day 0 and to $87.1 \pm 1.7$ % at day 5.

Figure 2 shows a typical $^{31}P$ NMR spectrum of $\beta$TC3 cells entrapped in APA beads and perfused with growth medium. To ensure the validity of our NMR results, inversion recovery experiments were performed to measure the $t_1$ values of the $\beta$-NTPs and the combined intracellular and extracellular $P_i$ [$P_{i(total)}$] resonances. Our measurements demonstrate that the $t_1$ value for the $\beta$-NTP resonance was not affected by the changes in glucose concentration ($0.50 \pm 0.02$ s at 0 mM and $0.52 \pm 0.05$ s at 16 mM). The $t_1$ value for the $P_{i(total)}$ resonance at 16 mM was

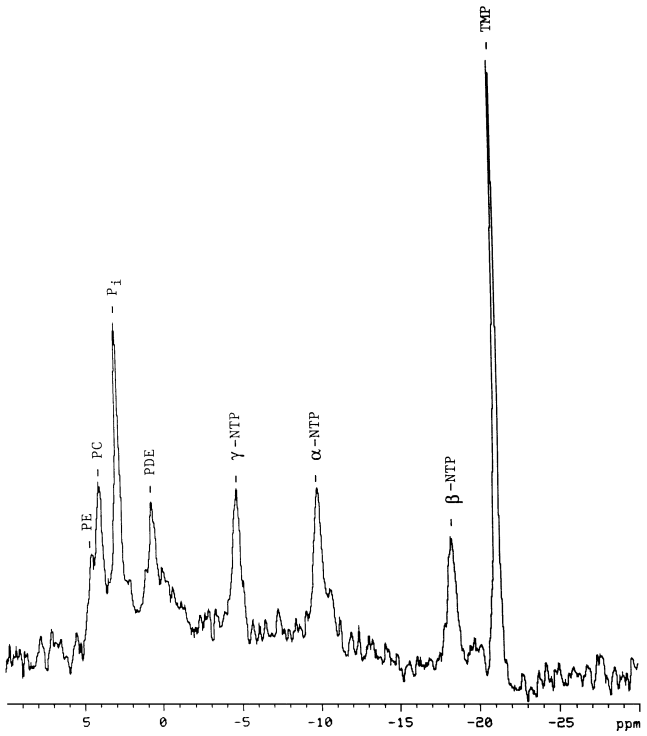


**Figure 2 Typical $^{31}$P NMR spectrum of $\beta$TC3 cells entrapped in APA beads and perfused with growth medium**

The spectrum was acquired over 27 min. Resonance assignments are as follows: PC, phosphocholine; PE, phosphoethanolamine; PDE, phosphodiesters; $\alpha$-, $\beta$- and $\gamma$-NTP, $\alpha$-, $\beta$- and $\gamma$-phosphates respectively of NTPs; TMP, trisodium trimetaphosphate.

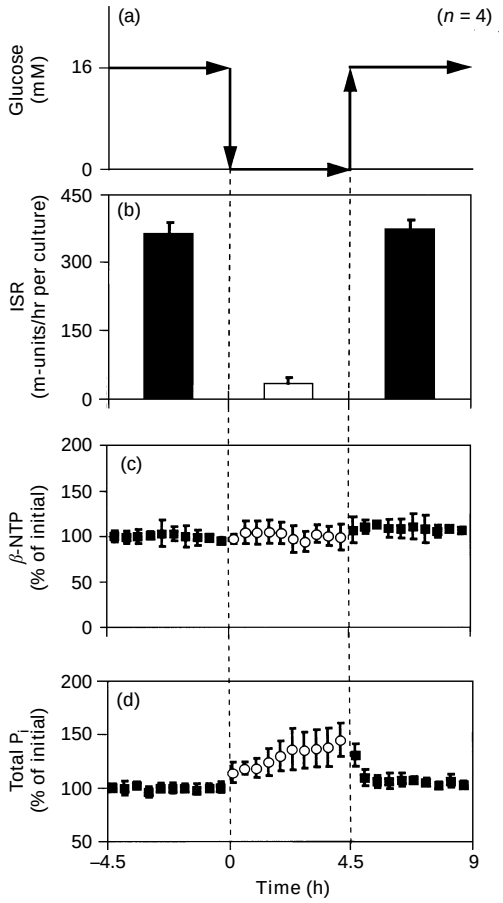


**Figure 3 Changes in IRP secretion rate, NTP and $P_{i(total)}$ as a function of time during the 16–0–16 mM glucose concentration step changes**

The results are from one of three cultures examined. There were four glucose concentration step changes in this culture, so data represent the averages of these episodes. (**a**) Schematic representation of the 16–0–16 mM glucose concentration step changes. (**b**) Average IRP secretion rates (ISR) determined over the 4.5 h periods prior to, during and after the 0 mM glucose episode. Error bars represent the S.D. of the rates measured for the four episodes performed in the culture. Errors due to repeated assays were propagated and were incorporated in the calculations. (**c**) Temporal profile of the $\beta$-NTP resonance during the glucose concentration step changes. Each point is the average of four values measured at the same time relative to the beginning of each basal episode. The error bars represent the S.D. (**d**) Temporal changes of the $P_{i(total)}$ resonance during the glucose concentration step changes. Data points were acquired and processed in exactly the same way as for the NTP data in (**c**). For reasons of clarity, all data points at 0 mM glucose are presented as open circles.

$4.7 \pm 0.5$ s; however, an accurate value at 0 mM glucose could not be determined because of the long $t_1$ relative to the duration of the basal episodes.

Changes in IRP secretion and in NTP and $P_{i(total)}$ concentrations measured during the step changes in glucose concentration are shown in Figure 3 for one of the three cultures. For clarity, data collected during the four episodes performed in this 5-day-long experiment are averaged and displayed as a single 16–0–16 mM glucose sequence (Figure 3a). Data acquired during the 4.5 h perfusion with 16 mM glucose prior to each zero-glucose episode are averaged and presented in the first segment ($-4.5$ to 0 h). Data acquired during each 0 mM glucose period are averaged and presented in the second segment (0–4.5 h), and data acquired during the 4.5 h after the initiation of reperfusion with 16 mM glucose are averaged and presented in the third segment (4.5–9 h).

Figure 3(b) shows the average IRP secretion rates measured during these three segments. Glucose-stimulated insulin secretion was achieved after every basal episode. The average rate of IRP secretion at 16 mM glucose was $338 \pm 42$ m-units/h per culture, and that at 0 mM glucose was $38 \pm 15$ m-units/h per culture.

The relative changes in the $\beta$-NTP peak area during the 16–0–16 mM step changes in glucose concentration are shown in Figure 3(c). The data are expressed as percentages of the initial concentration, which is defined as the average value derived over the 4.5 h period prior to the first 0 mM glucose episode. The initial intracellular concentration of NTP in entrapped $\beta$TC3 cells was $3.3 \pm 0.4$ $\mu$mol/culture. This value was obtained by taking the ratio of the areas under the $\beta$-NTP and trimetaphosphate resonances, and taking into account the biovolume, the volume of trimetaphosphate and the concentration of trimetaphosphate. Our data demonstrate that the intracellular NTP concentration was stable throughout the duration of these experiments, and that it was not affected by the step changes in glucose concentration, despite a significant change in the rate of IRP secretion. Because of the low $t_1$ value of the $\beta$-NTP resonance ($\sim 0.5$ s) relative to the 3.171 s inter-pulse delay in our acquisition parameters, $\beta$-NTP was fully relaxed in all acquired spectra. Therefore intracellular NTP concentrations calculated from the NMR spectra were not influenced by relaxation effects. Figure 3(d) shows the profile of $P_{i(total)}$ during the 16–0–16 mM step changes in glucose concentration. An increase in $P_{i(total)}$ during exposure to 0 mM glucose was observed.

In the absence of glucose, it was observed that the pH of the perfusion medium became more alkaline, resulting in the splitting

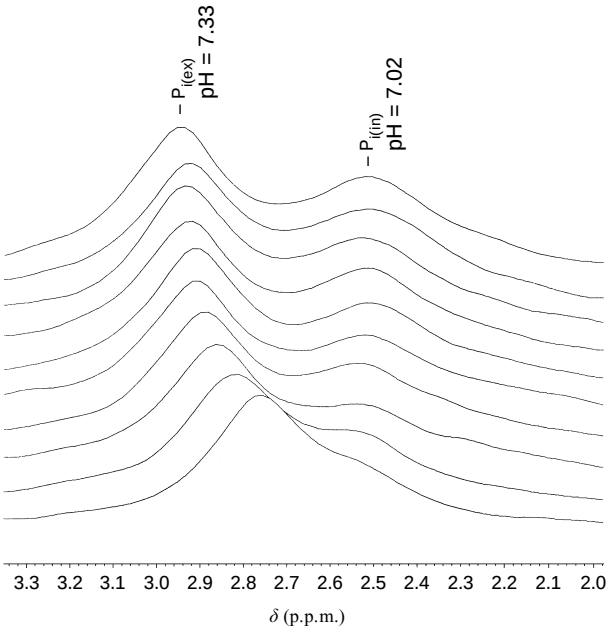


**Figure 4 Stack plot of $^{31}$P NMR spectra expanded over the $P_i$ region during a single 4.5 h exposure to 0 mM glucose**

Each spectrum was acquired over 27 min.

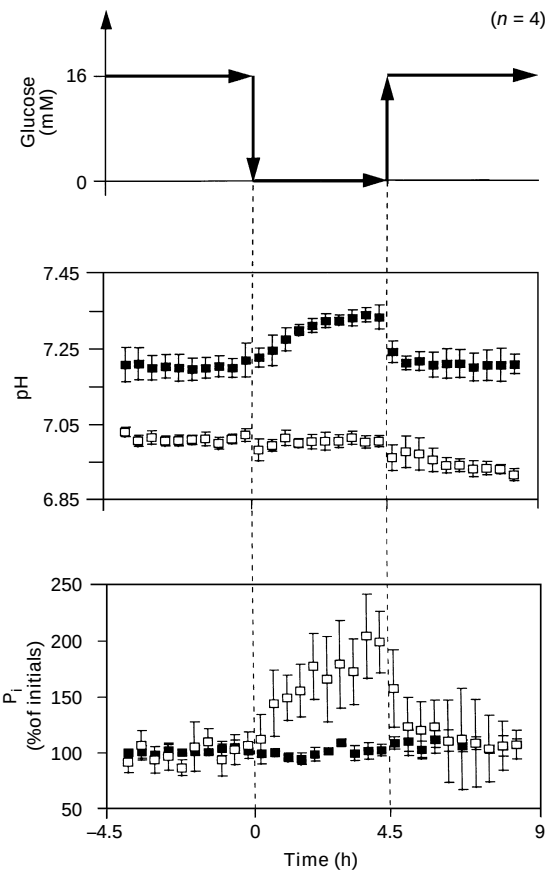


**Figure 5 Changes in intracellular and extracellular pH and $P_i$ as a function of time during the 16–0–16 mM glucose concentration step changes**

Results are from one of three cultures examined. Top: schematic representation of the 16–0–16 mM glucose concentration step changes. Middle: temporal changes in the NMR-detectable pH during the glucose concentration step changes: ■, extracellular pH; □, intracellular pH. Bottom: temporal changes in the two detectable $P_i$ pools during the glucose concentration step changes: ■, $P_{i(ex)}$; □, $P_{i(in)}$.

of the $P_i$ peak into two detectable resonances. This shift in medium pH was observed in all zero-glucose episodes, and was attributed to the significantly lower lactate and higher ammonia production in the glucose-free environment which could not be neutralized by the buffering capacity of the media. Figure 4 shows a stack plot of $^{31}$P NMR spectra (expanded over the $P_i$ chemical shift) acquired over the 4.5 h of exposure to 0 mM glucose, demonstrating the two $P_i$ pools. The spectral resolution is such that quantification of the two $P_i$ pools can be attained. The upfield resonance that corresponds to a more acidic environment is attributed to intracellular $P_i$ [$P_{i(in)}$], while the downfield resonance that corresponds to a more alkaline environment is attributed to extracellular $P_i$ [$P_{i(ex)}$].

Figure 5 shows the effect of the basal episodes on intra- and extra-cellular pH, and the concentrations of $P_{i(in)}$ and $P_{i(ex)}$. The data are displayed and averaged in the same manner as in Figure 3. Figure 5 (top panel) is a schematic of a single 16–0–16 mM glucose episode, while the middle and bottom panels illustrate the effects of glucose concentration on pH and $P_i$ respectively. Intracellular pH was maintained stable at $7.02 \pm 0.05$ throughout the step changes, while the extracellular pH displayed a transient increase from 7.15 to 7.35 during the 4.5 h exposure to glucose-free medium. Concomitantly, $P_{i(in)}$ doubled in concentration, while $P_{i(ex)}$ remained stable. $P_{i(in)}$ returned to its original level within 2 h after reperfusing with the high-glucose medium. Although it is not clear whether the observed changes in $P_{i(in)}$ are due to a biochemical change or to $t_1$, it is unlikely that $t_1$ is the main contributing factor for the following reason. Assuming that $t_1$ is solely responsible for the changes in $P_{i(in)}$, and that the spin-spin relaxation time ($t_2$) $\ll t_1$, then by using the following equation:

$$M_z = M_o(1 - e^{-t/t_1})$$

where $M_z$ is the longitudinal magnetization at an interpulse delay time $t$, $M_o$ is the equilibrium magnetization at an infinite delay time, and $t_1$ is the longitudinal relaxation time, we may determine the change in $t_1$ needed to account for the observed doubling of $P_{i(in)}$. If we assume that the $t_1$ value for $P_{i(in)}$ at 16 mM glucose is the same as that for $P_{i(total)}$, then $t_1$ would have to decrease from 4.7 s to 0.8 s. This is too large a change in $t_1$ for a minimal change in the intracellular ionic environment. In addition, if we use the $t_1$ value determined for $P_{i(in)}$ in C6 glioma cells exposed to a high glucose concentration ($t_1 = 2.0$ s) [19], then it is impossible to attribute the doubling of $P_{i(in)}$ solely to a change in $t_1$. Therefore the observed changes in $P_{i(in)}$ should be attributed mainly to a concentration change.

Measurements of the dissolved oxygen concentrations upstream and downstream of the bioreactor were made throughout the experiment. The rate of oxygen consumption by entrapped $\beta$TC3 cells was calculated by taking the difference between these measurements and multiplying it by the flow rate of the perfusion medium. The oxygen consumption rate was stable at $87 \pm 2$ $\mu$mol/h per culture, and was not affected by the glucose step changes. Our data are in agreement with an earlier report showing that the rate of oxygen consumption by entrapped $\beta$TC3 cells was not affected by similar glucose step changes [6].

Rates of glucose consumption, lactate production and ammonia production by the entrapped $\beta$TC3 cells were determined

**Table 1 Summary of data collected from all episodes performed during the three NMR experiments**

The data are presented as percentages of the values measured in the 4.5 h interval prior to each 0 mM glucose episode. Reported values represent means ± S.D. for all episodes measured. ND, not determined.

| | 16 mM Glucose | 0 mM Glucose | 16 mM Glucose |
|---|---|---|---|
| NTP concn. ($n = 10$) | 100 ± 12 | 93 ± 17 | 104 ± 4 |
| $P_{i(in)}$ concn. ($n = 10$) | 100 ± 2 | 170 ± 40 | 117 ± 24 |
| $P_{i(ex)}$ concn. ($n = 10$) | 100 ± 2 | 98 ± 3 | 103 ± 7 |
| IRP secretion rate ($n = 10$) | 100 ± 4 | 11 ± 9 | 97 ± 8 |
| Oxygen consumption rate ($n = 2$) | 100 ± 2 | 102 ± 5 | 101 ± 10 |
| Glucose consumption rate ($n = 10$) | 100 ± 22 | ND | 109 ± 10 |
| Lactate production rate ($n = 2$) | 100 ± 17 | 24 ± 1 | 103 ± 13 |
| Ammonia production rate ($n = 2$) | 100 ± 20 | 194 ± 25 | 112 ± 4 |

**Table 2 Summary of data obtained from monolayer cultures exposed for 4 h to DMEM containing 25 mM or 0 mM glucose**

The values correspond to means ± S.D. of four flasks. ND, not determined.

| | 25 mM glucose | 0 mM glucose |
|---|---|---|
| IRP secretion rate ($\mu$-units/h per $10^5$ cells) | 59.6 ± 4.7 | 5.8 ± 5.2 |
| Ammonia production rate (nmol/h per $10^5$ cells) | 4.8 ± 0.8 | 8.3 ± 0.4 |
| ATP concn. (nmol/$10^6$ cells) | 3.17 ± 0.29 | 3.15 ± 0.20 |
| Glucose consumption rate (nmol/h per $10^5$ cells) | 6.1 ± 0.3 | ND |
| Lactate production rate (nmol/h per $10^5$ cells) | 7.9 ± 0.5 | ND |

periodically throughout the experiment. Table 1 summarizes the changes in NTP, $P_{i(in)}$ and $P_{i(ex)}$, and of the measured metabolic and secretory rates of entrapped $\beta$TC3 cells.

To confirm the results obtained by NMR spectroscopy, a set of monolayer experiments was also performed in which ATP was measured in cell extracts. Table 2 shows the results from a set of monolayer cultures exposed for 4 h to DMEM containing either 25 mM or 0 mM glucose. The absence of glucose from the medium caused an approx. 10-fold decrease in IRP secretion and a 2-fold increase in ammonia production, but did not affect the intracellular ATP concentration. Cell viability at the end of the 4 h basal episode was also unaffected by the glucose-free environment.

## DISCUSSION

The biochemical mechanism by which changes in the extracellular glucose concentration are translated into changes in insulin secretion is the subject of intense investigation. A link between glucose metabolism and insulin exocytosis has been postulated. This link, known as the Fuel Hypothesis, is based primarily on islet metabolism, and it is unclear whether it is valid for transformed $\beta$ cell lines. These cell lines are important to diabetes research, since they are considered as possible alternatives to islets in the development of a cell-based bioartificial pancreas. To investigate the Fuel Hypothesis in a transformed $\beta$ cell line, we used mouse insulinoma $\beta$TC3 cells entrapped in APA beads and as monolayer cultures, and we monitored their bioenergetic status and specific metabolic and secretory rates.

Basal episodes were performed at 0 mM glucose, because of the hypersensitivity of the $\beta$TC3 cells to glucose. The half-maximal secretory response in $\beta$TC3 cells occurs at 0.1–0.2 mM glucose, rather than 8 mM as is the case in normal islets [20,21]. Entrapped $\beta$TC3 cells responded repetitively to glucose concentration step changes over a 5-day period. A 10-fold decrease in insulin secretion was measured during all 0 mM glucose episodes. The same 10-fold decrease in IRP secretion was also measured in the monolayer cultures exposed to 0 mM glucose.

Our data demonstrated that episodes of 0 mM glucose had no significant effect on the intracellular NTP concentration or the rate of oxygen consumption by APA-entrapped and monolayer $\beta$TC3 cell cultures, despite a 10-fold change in the rate of IRP secretion. This invariance in NTP and oxygen consumption shows that exposure to 0 mM glucose for 4.5 h did not cause nutrient starvation of the cells. Available literature on islet and transformed $\beta$ cell biochemistry is inconclusive about a correlation between intracellular ATP concentration and changes in glucose concentration. With regard to islets, the inconsistencies among results may be attributed, in part, to the differences in experimental approaches used. When experiments have been performed by preincubating islets in media containing substimulatory levels of glucose but supplemented with other fuels, a correlation was not observed [22–28]; alternatively, when islets were preincubated in media without glucose or other fuels, a positive correlation was demonstrated [25,29–31].

With regard to transformed $\beta$ cells, the available literature is inconclusive as to whether a correlation exists between ATP and insulin secretion. Results reported by Matschinsky [32] with $\beta$HC9 and $\beta$TC3 cells entrapped in agarose beads appear to be in agreement with our observations. In that study, entrapped cells were perfused with an unspecified medium containing high concentrations of phosphocreatine to aid in the determination of the free intracellular ADP concentration. Switching the perfusion medium from one containing a low glucose concentration (0.2 mM for $\beta$TC3 cells or 3 mM for $\beta$HC9 cells) to one containing 25 mM glucose resulted in a decrease in the free ADP concentration from 35 $\mu$M to 20 $\mu$M in both cell lines, whereas the NMR-detectable ATP remained constant throughout the glucose concentration step change [32]. In another investigation with the same cell lines, Liang et al. calculated the rate of ATP biosynthesis as a function of glucose concentration [33]. These calculations were based on a series of enzymic assays performed on cells exposed to a modified Hanks salt buffer containing different glucose concentrations but no other fuels. The authors demonstrated that in both cell lines the rate of ATP production increased with increasing glucose concentration. However, the total ATP concentration was not reported. Although it has been hypothesized that the rate of ATP consumption is also positively correlated with the glucose concentration, the magnitude of this rate and thus the concentration of free intracellular ATP are unknown [11,32].

In another NMR-based study, RINm5F cells cultured in microcarrier beads and perfused with DMEM displayed a 100 % decline in the ATP concentration within 30 min of exposure to basal conditions (0 mM glucose) [34]. The authors attributed these ATP changes to the process of insulin secretion. However, the validity of this conclusion is doubtful, for the following reasons. Firstly, no data were reported on insulin secretion by RINm5F cells during these step changes. This is particularly important, since it is not established that RINm5F cells are glucose-responsive [30,31,35,36]. Secondly, careful analysis of the reported experimental parameters reveals that the cells were most likely maintained under hypoxic or even anoxic conditions [37]. Since hypoxia results in a decrease in ATP levels, de-

convolution of the contributions of hypoxia and hypoglycaemia is impossible. Furthermore, in experiments performed in our laboratory with APA-entrapped RINm5F cells perfused with DMEM supplemented with sera and glutamine under well oxygenated conditions, we failed to detect significant changes in NTP levels with step changes in glucose concentration [37].

A possible cause of the invariance of the NTP concentration during our experiments was an increase in glutamine utilization during the episodes of 0 mM glucose. This hypothesis is supported by the increase in ammonia production during each basal episode (Tables 1 and 2). In experiments on islets fed with glucose-free media, a similar increase in ammonia production was observed [29]. The use of glutamine as the primary source of fuel under conditions of glucose starvation has been demonstrated for a variety of normal and transformed cells [38–40]. It has been shown that, when cells are well oxygenated, glutamine can maintain their ATP levels in the absence of glucose for at least 4 h, and in some cases even up to 24 h [38–40]. However, when hypoxic or anoxic conditions prevail, glutamine can no longer do this [39,40].

Under conditions of glucose-stimulated insulin secretion, islets exhibit an increase in their rate of oxygen consumption. This has been attributed, in part, to the increased energy requirement due to insulin secretion and/or biosynthesis [41,42]. Such a correlation, however, may not exist for $\beta$TC3 cells, since their insulin content is an order of magnitude smaller than that of islets [9,20,43], whereas their intracellular ATP concentration is similar to that of islets [11,44]. Consequently, the energy requirement for insulin biosynthesis and secretion may be smaller on a per cell basis for $\beta$TC3 cells, and it may involve a smaller fraction of intracellular NTP than in islets. The stability of the rate of oxygen consumption observed in the present study is in agreement with the concomitant stability of the intracellular NTP concentration. In contrast with our observation are the report by Liang et al. [33], in which oxygen consumption increased with glucose concentration in $\beta$TC3 and $\beta$HC9 cells, and the studies with RINm5F cells [30,31,36], in which oxygen consumption increased as the cells were switched from 0 mM to 2.8 mM glucose. This discrepancy may be attributed to the differences in culture conditions in the various experiments. In our study, $\beta$TC3 cells were always exposed to a nutrient-rich environment, regardless of the glucose concentration, whereas in the studies of Liang et al. [33] and Sener et al. [30,31,36] cells were preincubated in a nutrient-free buffer for 20–30 min before stimulation.

The increase in the $P_{i(in)}$ concentration observed under basal conditions in entrapped $\beta$TC3 cells is in agreement with the '$P_i$ flush' noted under stimulated conditions in islets [11,45,46], and with the involvement of the ATP mass action ratio ($ATP/ADP \cdot P_i$) in insulin release [10,32,33,46]. However, it disagrees with the study of Ghosh et al. [22], in which an increase in $P_i$ concentration was observed during the stimulation of insulin secretion. The mechanism for the rapid efflux of $P_{i(in)}$ is not well understood. It has been suggested that nutrient secretagogues may alter the permeability of the cell membrane to ions, or that $P_i$ is sequestered in secretory granules and released simultaneously with insulin [11]. The involvement of $P_i$ in the secretory cascade of islets was suggested by Ohta et al. [46], who demonstrated that stimulated insulin release was inhibited by an increase in the $P_{i(in)}$ concentration. However, the mechanism for this action is still obscure. It is unlikely that $P_i$ is directly responsible for the regulation of the ATP-sensitive $K^+$ channels. The available information suggests that these channels may be regulated by changes in the ATP mass action ratio, of which $P_i$ is a part, rather than by $P_i$ alone. Unfortunately, intracellular ADP could not be measured with our experimental set-up; therefore conclusions about its involvement in stimulated secretion cannot be reached.

Our observations that step changes in the extracellular glucose concentration do not affect intracellular NTP and oxygen consumption, but do affect $P_{i(in)}$, are of significance to the mechanism of the Fuel Hypothesis in $\beta$ cell lines. It is thought that an important intermediate step in this mechanism is the increase in oxygen consumption and the resultant increase in the ATP mass action ratio. Our results show that, for $\beta$TC3 cells, neither oxygen consumption nor the total intracellular ATP concentration are important signalling intermediates, whereas the changes in $P_{i(in)}$ are consistent with the hypothesis that the ATP mass action ratio increases upon glucose stimulation and thus represents a possible link between glucose metabolism and the electrophysiological events associated with secretion.

This work was supported in part by grants from NIH (DK47858), NSF (BES-9410703), and the Georgia Research Alliance. Their financial support is greatly appreciated. We also acknowledge Ms. Inge Rask for her excellent technical support.

## REFERENCES


1 Lim, F. and Sun, A. M. (1980) Science **210**, 908–910
2 Soon-Shiong, P., Heintz, R. E., Merideth, N., Yao, Q. X., Yao, Z., Murphy, M., Moloney, M. K., Schmehl, M., Harris, M., Mendez, R. and Sanford, P. A. (1994) Lancet **343**, 950–951
3 Lacy, P. E., Hegre, O. D., Gerasimidi-Vazeou, A., Gentile, F. T. and Dionne, K. E. (1991) Science **254**, 1782–1784
4 Lanza, R. P., Butler, D. H., Borland, K. M., Staruk, J. E., Faustman, D. L., Solomon, B. A., Muller, T. E., Rupp, R. G., Maki, T., Monaco, A. P. and Chick, W. L. (1991) Proc. Natl. Acad. Sci. U.S.A. **88**, 11100–11104
5 Lanza, R. P., Ecker, D., Kuhtreiber, W. M., Staruk, J. E., Marsh, J. and Chick, W. L. (1995) Transplantation **59**, 1485–1487
6 Mukundan, N. E., Flanders, P. C., Constantinidis, I., Papas, K. K. and Sambanis, A. (1995) Biochem. Biophys. Res. Commun. **210**, 113–118
7 Sambanis, A., Papas, K. K., Flanders, P. C., Long, Jr., R. C., Kang, H. and Constantinidis, I. (1994) Cytotechnology **15**, 351–363
8 Ohgawara, H., Miyazaki, J., Karibe, S., Tashiro, F., Akaike, T. and Hashimoto, Y. (1995) Cell Transplant. **4**, 307–313
9 Efrat, S., Linde, S., Kofod, H., Spector, D., Delannoy, M., Grant, S., Hanahan, D. and Baekkeskov, S. (1988) Proc. Natl. Acad. Sci. U.S.A. **85**, 9037–9041
10 Liang, Y. and Matschinsky, F. M. (1994) Annu. Rev. Nutr. **14**, 59–81
11 Erecinska, M., Bryla, J., Michalik, M., Meglasson, M. D. and Nelson, D. (1992) Biochim. Biophys. Acta **1101**, 273–295
12 Meglasson, M. D. and Matschinsky, F. M. (1984) Am. J. Physiol. **246**, E1–E13
13 Newgard, C. B. and McGarry, J. D. (1995) Annu. Rev. Biochem. **64**, 689–719
14 Constantinidis, I. and Sambanis, A. (1995) Biotechnol. Bioeng. **47**, 431–443
15 Evanochko, W. T., Sakai, T. T., Ng, T. C., Krishna, N. R., Kim, H. D., Zeidler, R. B., Ghanta, V. K., Brockman, R. W., Schiffer, L. M., Braunschweiger, P. G. and Glickson, J. D. (1984) Biochim. Biophys. Acta **805**, 104–116
16 Sun, A. M., Parisius, W., Macmorine, H., Sefton, M. V. and Stone, R. (1980) Artif. Organs **4**, 275–278
17 Chang, L.-H., Chew, W. M., Weinstein, P. R. and James, T. L. (1987) J. Magn. Reson. **72**, 168–172
18 Schnall, M. D., Subramanian, V. H., Leigh, J. S. and Chance, B. (1985) J. Magn. Reson. **65**, 122–129
19 Merle, M., Pianet, I., Canioni, P. and Labouesse, J. (1992) Biochimie **74**, 919–930
20 Grampp, G. E. (1992) Ph.D. Thesis, Massachusetts Institute of Technology, Boston
21 Tal, M., Thorens, B., Surana, M., Fleischer, N., Lodish, H. F., Hanahan, D. and Efrat, S. (1992) Mol. Cell. Biol. **12**, 422–432
22 Ghosh, A., Ronner, P., Cheong, E., Khalid, P. and Matschinsky, F. M. (1991) J. Biol. Chem. **266**, 22887–22892
23 Matschinsky, F. M. and Ellerman, J. E. (1968) J. Biol. Chem. **243**, 2730–2736
24 Matschinsky, F. M., Ellerman, J. E., Krzanowski, J., Kotler-Brajtburg, J., Landgraf, R. and Fertel, R. (1971) J. Biol. Chem. **246**, 1007–1011
25 Matschinsky, F. M., Landgraf, R., Ellerman, J. and Kotler-Brajtburg, J. (1972) Diabetes **21**, 555–569
26 Meglasson, M. D., Nelson, J., Nelson, D. and Erecinska, M. (1989) Metab. Clin. Exp. **38**, 1188–1195
27 Trus, M. D., Zawalich, W. S., Burch, P. T., Berner, D. K., Weill, V. A. and Matschinsky, F. M. (1981) Diabetes **30**, 911–922

28 Malaisse, W. J. and Sener, A. (1987) Biochim. Biophys. Acta **927**, 190–195
29 Malaisse, W. J., Best, L., Kawazu, S., Malaisse-Lagaae, F. and Sener, A. (1983) Arch. Biochem. Biophys. **224**, 102–110
30 Sener, A., Giroix, M. H., Hellerstrom, C. and Malaisse, W. J. (1987) Cancer Res. **47**, 5905–5907
31 Sener, A., Leclercq-Meyer, V., Giroix, M. H., Malaisse, W. J. and Hellerstrom, C. (1987) Diabetes **36**, 187–192
32 Matschinsky, F. M. (1996) Diabetes **45**, 223–241
33 Liang, Y., Bai, G., Doliba, N., Buettger, C., Wang, L., Berner, D. K. and Matschinsky, F. M. (1996) Am. J. Physiol. **270**, E846–E857
34 Kriat, M., Fantini, J., Viom-Dury, J., Confort-Gouny, S., Galons, J. P. and Cozzonne, P. J. (1992) Biochimie **74**, 949–955
35 Halban, P. A., Praz, G. A. and Wollheim, C. B. (1983) Biochem. J. **212**, 439–443
36 Sener, A., Blachier, F. and Malaisse, W. J. (1988) J. Biol. Chem. **263**, 1904–1909
37 Papas, K. K. (1996) Ph.D. Thesis, Georgia Institute of Technology, Atlanta, GA
38 Pauwels, P. J., Opperdoes, F. R. and Trouet, A. (1984) J. Neurochem. **44**, 143–148
39 Reitzer, L. J., Wise, B. M. and Kennell, D. (1979) J. Biol. Chem. **254**, 2669–2676
40 Pianet, I., Merle, M., Labouesse, J. and Canioni, P. (1991) Eur. J. Biochem. **195**, 87–95
41 Hutton, J. C. and Malaisse, W. J. (1980) Diabetologia **18**, 395–405
42 Panten, U., Zunkler, B. J., Scheit, S., Kirchhoff, K. and Lenzen, S. (1986) Diabetologia **29**, 648–654
43 Efrat, S., Leiser, M., Surana, M., Tal, M., Fusco-Damane, D. and Fleischer, N. (1993) Diabetes **42**, 901–907
44 Ohta, M., Nelson, D., Nelson, J., Meglasson, M. D. and Erecinska, M. (1990) J. Biol. Chem. **265**, 17525–17532
45 Freinkel, N., Younsi, C. E., Bonnar, J. and Dawson, R. M. C. (1974) J. Clin. Invest. **54**, 1179–1189
46 Ohta, M., Nelson, D., Wilson, J. M., Meglasson, M. D. and Erecinska, M. (1992) Biochem. Pharmacol. **43**, 1859–1864

Received 16 December 1996/26 February 1997; accepted 25 March 1997